LOI to JLab PAC31

RF Cherenkov picosecond timing technique for Jlab 12 GeV physics program

A. Margaryan[1], O. Hashimoto[2], S. Majewski[3], L. Tang[3]

[1] *Yerevan Physics Institute, 375036 Yerevan, Armenia*
[2] *Tohoku University, Sendai, 98-77, Japan*
[3]*Thomas Jefferson National Accelerator Facility, Newport News, VA 23606, USA*

Abstract: A new particle identification device for Jlab 12 GeV physics program is proposed. It is based on the measurement of time information by means of a new radio frequency picosecond phototube (RFPP) and time measuring concept. The expected time measurement precision for Cherenkov time-of-flight (TOF) detector in a "head-on" geometry based on RFPP is about or less than 5 picoseconds, FWHM.
The proposal has two goals,

1. The R&D for optimization and manufacturing of the RFPP.
2. The development, construction and test of a Cherenkov picosecond timing technique based on the RFPP, for Jlab 12 GeV physics program, in particular, the development of Cherenkov correlated timing (CCT) or time-of-propagation detector (TOP) and Cherenkov TOF detector in a "head-on" geometry. It is supposed that the RFPP will be manufactured by the US company and that the prototype Cherenkov detectors will be constructed at Yerevan, tested at Yerevan and at Tohoku University electron stretcher-booster and latter at JLab.

1. Introduction

At present the photon detection is carried out with solid state devices, vacuum photomultiplier tubes (PMTs) or hybrid photon detectors (HPDs). These instruments also provide fast time information necessary in different fields of science and engineering. In the high energy particle physics and nuclear physics experiments the time precision limit for the current systems consisting of particle detectors based on PMTs or HPDs and common nanosecond electronics (amplifiers, discriminators, logic units and time-to-digital converters) is about 100 ps (FWHM). A micro-channel plate (MCP) photo-multiplier tube generally provides good timing resolution. The transit time spread of the best MCP phototube is σ_{TTS} = 30–40 ps [1].

However, it is well known that timing systems based on radio frequency (RF) fields can provide precision of the order of 1 ps or better [2-4]. Streak cameras, based on similar principles, are used routinely for time measurements in the picosecond range and have found an increasing number of applications, in particular, in particle accelerators, permitting both precise measurements and instructive visualizations of beam characteristics and behavior that cannot be obtained using other beam instrumentation [5]. With a streak camera operating in the repetitive mode known as “synchroscan”, a typical temporal resolution of 2 ps (FWHM) can be reached for a long time exposure (more than one hour) [5, 6]. Nevertheless, the RF timing technique as well as the streak cameras did not find in the past wide application, including the elementary particle physics and nuclear physics experiments.

The basic principle of the RF timing technique or streak camera’s operation is the conversion of the time domain information into spatial one by means of RF fields.

Recently we have developed an RF picosecond phototube (RFPP) [7,8], based on the 500 MHz RF circular sweep deflector, which combines all advantages of a regular PMT and a circular scan streak camera. This kind of phototube is capable of detecting optical signals and providing nanosecond signals, like fast photomultiplier, for future event by event processing of each photoelectron with better than 20 ps resolution.

We propose to develop, construct and test Cherenkov time of flight detectors based on the RFPP for JLAB 12 GeV physics program.

We define the project with three phases as follows:

1. Phase 1: R&D for optimization of the parameters of 500 MHz RFPP and manufacturing of the RFPP.
2. Phase 2: Development, construction and test of the Cherenkov counters based on the RFPP in the lab.
3. Phase 3: Construction, test and operation of RF Cherenkov counter systems at JLab.

2. RF picosecond phototube: design feature

2.1 RFPP with point size photocathode and obtained results with thermo-electron source

The general layout of the proposed phototube [8] for point-size photocathode is shown in Fig. 1. The primary photon pulse hits the photocathode (1) and produces photo-electrons (PEs). These electrons are accelerated by a voltage V applied between the photocathode and an electron transparent electrode (2). The electrostatic lens (3) then focuses the electrons onto the screen (7) at the far end of the tube, were secondary electron (SE) detector is placed. The time structure of the produced PE bunch is identical to that of the light pulse. Along the way the electrons are deflected by the circular sweep RF deflection system, consisting of electrodes (4) and $\lambda/4$ coaxial RF cavity (6), which operates at 500 MHz and form a circle on the screen, where the time structure of the input photon signal is transferred into spatial PE image (5) and detected. By this way the timing error sources are minimized, because PEs is timed before the necessary further signal amplification and processing. The thermionically emitted electrons are distributed randomly and form a circle on the screen.

Several factors determine the time resolution of such a device:

1) **Physical time resolution of the photocathode, i.e., the time dispersion or delay of the photo-electrons.** A delay and time spread of the photoelectrons $\Delta\tau_p$ is caused by the finite thickness of the photocathode Δl and the energy spread of the $\Delta\varepsilon$ PEs. For the typical thickness of semitransparent bialkali photocathode, $\Delta l \cong 20nm$, and $\Delta\varepsilon = 1eV$ we obtain $\Delta\tau_p \le 10^{-12}\,s$.
2) **Physical time resolution of the electron tube.** The minimal time dispersion is determined by chromatic aberration due to the PEs' initial energy spread $\Delta\varepsilon$. The time spread in the case of a uniform accelerating electric field E near the photocathode, is $\Delta\tau_t = 1.7\times10^{-8}(\Delta\varepsilon)^{1/2}/E$ s, where $\Delta\varepsilon$ is in eV, and E is in V/cm [1, 8]. For our case, the applied voltage V = 2.5 keV, Z = 0.25 cm (see Fig. 1), and $E = 10kV/cm$. For $\Delta\varepsilon = 1eV$ we obtain $\Delta\tau_t \approx 2\times10^{-12}\,s$.
3) **Technical time resolution of the electron tube** is determined by the electron transit time dispersion and in a carefully designed system this time dispersion can be minimized to be in ps range.
4) **Technical time resolution of the RF deflector.** By definition the technical time resolution is $\Delta\tau_d = d/\nu$ where d is the size of the electron beam spot or the position resolution of the secondary electron detector (if the electron beam spot is smaller), while ν is the scanning speed: $\nu = 2\pi R/T$. Here T is the period of the RF field and R is the radius of the circular sweep on the position-sensitive detector. For example, if $T = 2\times10^{-9}$ s ($f = 500$ MHz), $R = 2$ cm, and $d = 1.0$ mm, we have $\nu \ge 0.5\times10^{10}\,cm/s$ and for time resolution get $\Delta\tau_d \le 20\times10^{-12}\,s$.

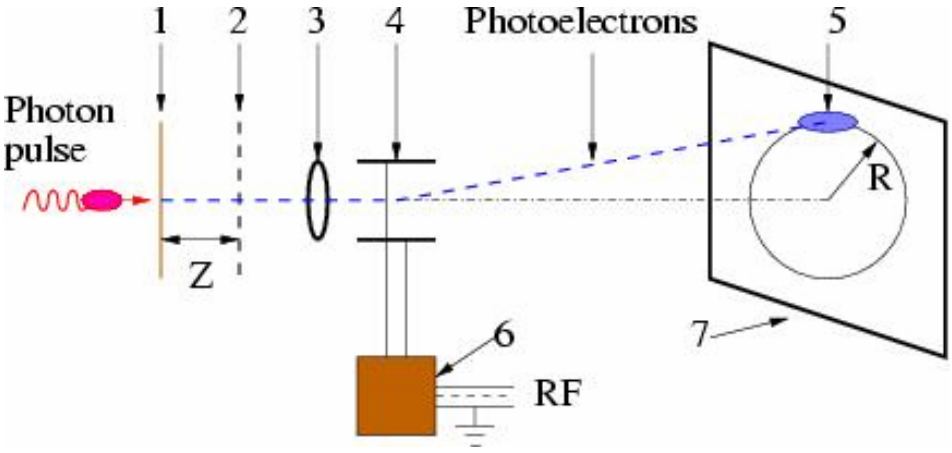

Figure 1: The schematic layout of the RF phototube with point-size photocathode.
1- photo-cathode, 2- electron transparent electrode, 3- electrostatic lens, 4- RF deflector, 5- image of photo electrons, 6- $\lambda/4$ coaxial RF cavity, 7- SE detector.

To scan circularly 2.5 keV electrons we have used a dedicated RF deflecting system developed by our group [7, 8] at a frequency of $f = 500$ MHz. This RF deflecting system consists of a $\lambda/4$ coaxial cavity and deflection electrodes. It is constructed in such a way that the deflection electrodes serve as a capacitance element which contains all the applied RF power localized inside. The deflection electrodes formed part of resonance circuit with a Q-factor of about 130. In addition the special design of the deflection electrodes allows avoiding transit time effects. The sensitivity of this new and compact RF deflector is about 1 mm/V or 0.1 $rad/W^{1/2}$ and is an order of magnitude higher than the sensitivities of the RF deflectors used previously. The experimental setup has been tested by using thermo-electrons emitted from the wire, when it is heated by a current. For visual tuning of the experimental setup a phosphor screen is situated at the far end of the electron tube. About 1 W (on $50\,\Omega$) RF power at 500 MHz has been used to scan the beam circularly and to reach 2 cm radius (see Fig. 2) or 20 ps resolution for 2.5 keV electrons. For comparison we note that in the reference [9] to reach 2 cm radius, 17 W RF power at 500 MHz was used.

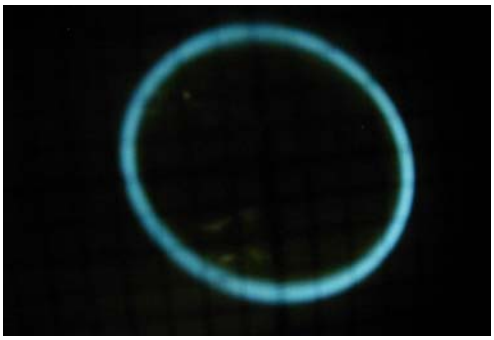

Figure 2: Image of circularly scanned 2.5 keV electron beam on the phosphor screen.

2.2 Photo-electron detector

The detection of the PEs is accomplished with position sensitive detector based on MCPs, the schematic of which is displayed in the Fig. 3.

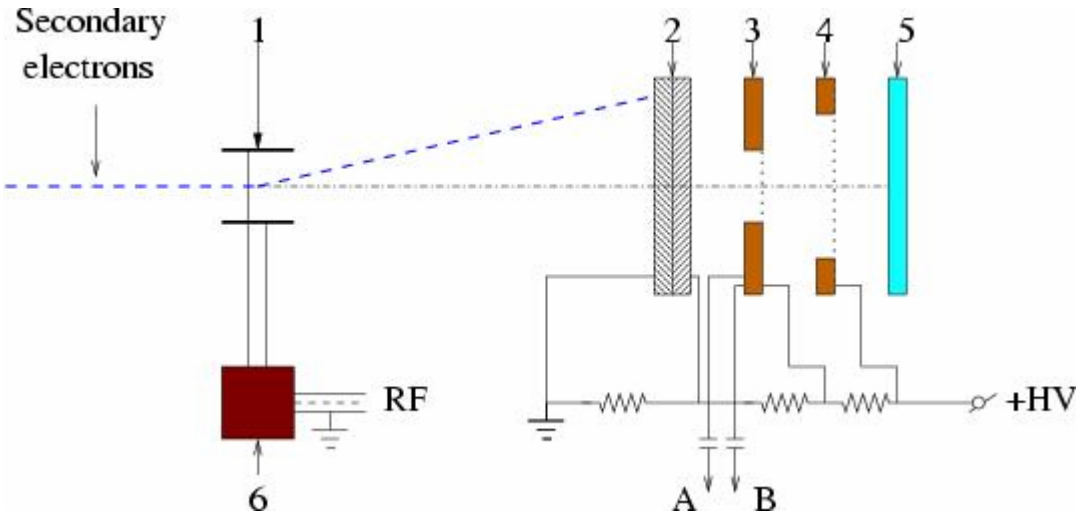

Figure 3: Schematic view of the position sensitive detector based on MCPs. 1- RF deflector, 2- MCPs, 3- position sensitive anode and accelerating electrode, 4- accelerating electrode, 5- phosphor screen, 6- quarter wavelength coaxial cavity, A and B are position signals.

A dual, chevron type, MCP detection system is used to obtain a high gain. Both MCPs are identical at 32 mm in diameter and can sustain a maximum bias of about 1000 VDC each. The dual MCP system has a combined maximum gain of about 10^7. The position sensitive resistive anode (Fig. 4) is situated about 3 mm behind the second MCP. It is biased at ~300V relative to the MCP output to allow electrons multiplied in the MCP reach the anode. To tune the system under visual control, the anode has a hole in the center and a phosphor screen is placed about 3 mm behind it. It is biased at ~2 kV relative to the MCP output to convert the accelerated electrons energy into visible photons. We use wire planes made of 2 mm thick G10 plates to feed the bias voltages. Both planes use 20 μm diameter gold-plated tungsten wires and have wire spacing of 1 mm. The visually tuned image of circularly scanned 2.5 keV electron beam amplified in the MCP is also displayed in the Fig. 4. The shadow of the wires of both electrodes is seen clearly and can be used to determine an absolute scale of the image. From the Fig. 4 it follows that the amplified beam's size is about 1 mm: therefore for R = 2 cm scanned circle, the time resolution for single SE is expected to be $\Delta\tau_d \le 20\times10^{-12}$ s.

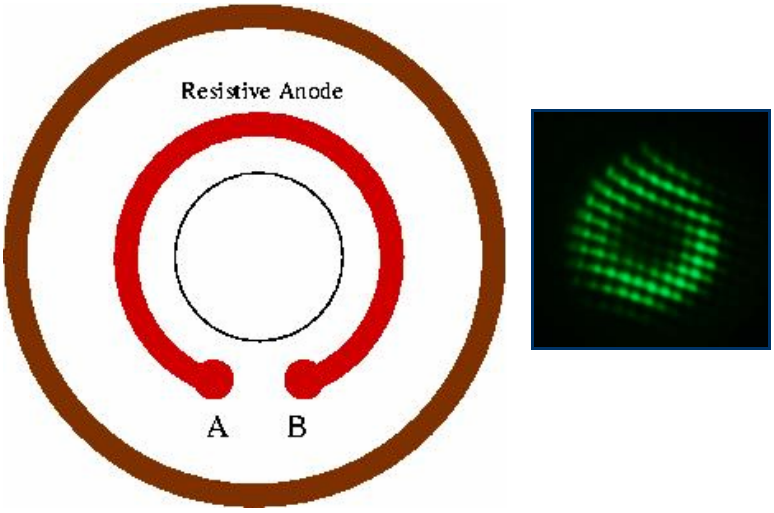

Figure 4: Schematic of the resistive anode and image of circularly scanned and amplified (in the MCP) 2.5 keV electron beam on the phosphor screen.

By increasing the RF power we fit the size of the scanned circle to the size of the position sensitive resistive anode. Then we decrease the intensity of the thermo electrons by decreasing the heating current, to be able to read event by event the signals A and B on the scope. Typical signal detected with a digital 400 MHz scope is shown in the Fig. 5. It consists of two parts: signal generated in MCP by circularly scanned 2.5 keV single electrons; and signal induced by the RF deflector's 500 MHz RF noise. One can see that the amplitude of the induced 500 MHz RF noise from ~0.5 W RF power is about an order of magnitude smaller than the amplitude of amplified in MCP signals of single SE.

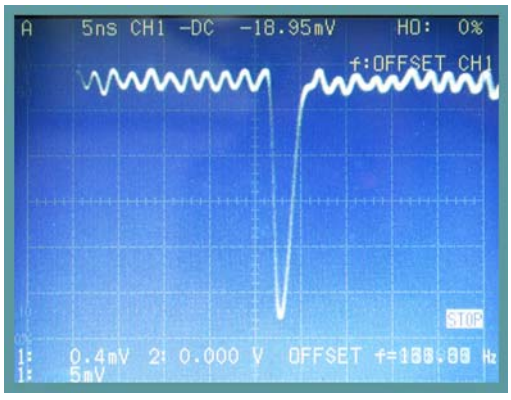

Figure 5: Photo of the oscilloscope's screen, showing scanned single SE signal from position sensitive anode.

Thus, signals from such a device can be processed by using common nanosecond-time electronics (amplifiers, discriminators, logic units, analog-to-digital converters and

etc.), and time resolution better than 20 ps can be achieved for single SE. The time resolution can be improved, if necessary, by using higher frequencies, since it is possible to operate the developed RF deflector and scan circularly keV electrons in the frequency range 500-1500 MHz.

By using direct readout scheme such as an array of small ($\sim 1mm^2$) pixels with one readout channel per pixel, the RFPP can be used as an optical waveform digitization device in the nanosecond and sub-nanosecond domain.

2.3 RFPP with large size photocathode

The general layout of the RF phototube with large-size photocathode, which is needed in high energy elementary particle physics and nuclear physics experiments, is shown in Fig. 6. We propose to use "spherical-capacitor" type immersion lens. It implies a configuration consisting of two concentric spheres of which the outer one is a photocathode (1) and the inner one is an electron transparent electrode (2). This configuration has a number of advantages, e.g., the possibility of having high accelerating field near the photocathode, between photocathode (1) and electrode (2), form a perfect crossover outside of this electric field and a complete lack of transit time dispersions in the crossover for electrons with equal initial energies. The transmission dynode (3) is placed in the crossover. In a tube with similar structure and with 40 mm diameter photocathode but without transmission dynode, 10 ps (FWHM) temporal resolution has been achieved [10]. The produced photoelectrons are accelerated in the "spherical-capacitor" region and focused on the crossover where they pass through transmission dynode (3) producing secondary electrons (SEs) on both sides of the dynode. Low energy SEs produced on the rear side of the transmission dynode are accelerated with the help of the electron transparent electrode (4) and enter into the electron tube which is the same as in the case of point size photocathode. Thus, with such a device, temporal resolution will be determined by the "spherical-capacitor" type immersion lens, because time dispersion of secondary electrons in the transmission dynode is less than 6 ps [11]. Hence, it becomes possible to attain a rather high temporal resolution for large size photocathode.

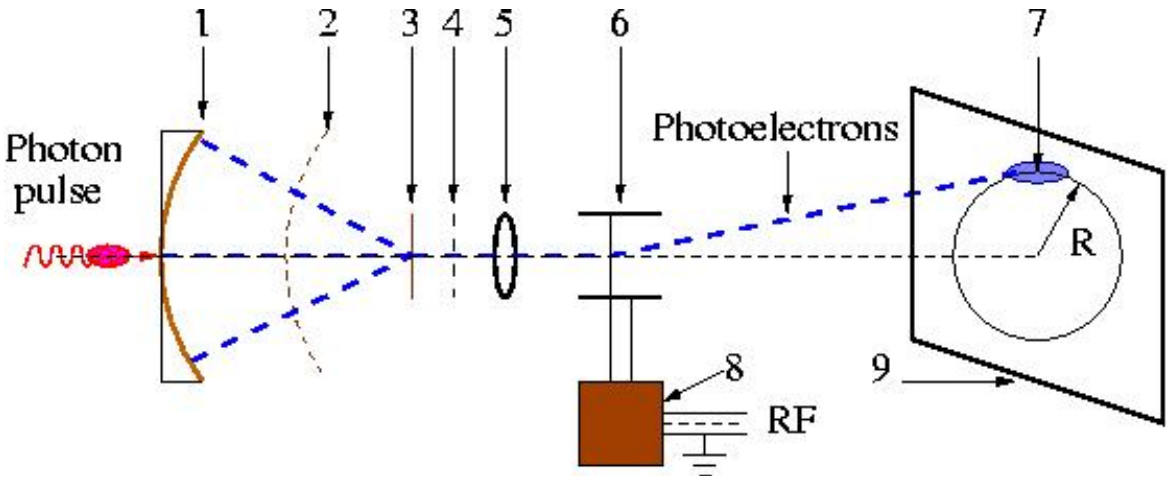

Figure 6: The schematic layout of the RF phototube with large size photocathode. 1- photo cathode, 2- electron transparent electrode, 3- transmission dynode, 4- accelerating electrode, 5-electrostatic lens, 6- RF deflection electrodes, 7- image of PEs, 8- $\lambda/4$ RF coaxial cavity, 9- SE detector.

3. Cherenkov TOF Detector Based on Picosecond Photon Technique

The time resolution of the TOF counter using plastic scintillators is inherently limited by the following effects besides the transit-time spread (TTS) of the phototube:

i) a finite decay time of photon emission;

ii) a different photon propagation-length or propagation-time in the scintillators to a phototube depending on the photon emission angle.

Thus the conventional TOF counter measures the arrival time of the earliest photons out of many, whereby the remaining large amount of photons are not effectively used for the time measurement.

By using Cherenkov radiation rather than the scintillation photons, two substantial and undesirable effects can be eliminated. While a decay constant of fast counting scintillator is typically ~2 ns, the flash duration of the Cherenkov radiation is ≤ 1ps [12]. While the propagation paths of scintillation photons are not unique due to uniform emission over 4π solid angle, they are unique for the Cherenkov radiation. The Cherenkov photon emission angle, θ_c, is uniquely determined by the particle velocity β. Depending on the particle, its momentum range, and experimental condition, there are various ways to do this using liquid, gas, or solid radiators with different type of photon detectors.

We will consider Cherenkov TOF detector in which the good time resolution is crucial [13]. Similar to the DIRC, Detection of Internally Reflected Cherenkov light [14], the Cherenkov TOF couples DIRC bar with a picosecond photon detector that times the photoelectrons seen at the end of the bar. In so doing, a DIRC utilizes the optical material of the radiator in two ways, simultaneously; first, as a Cherenkov radiator, and second, as a light pipe for the Cherenkov light trapped in the radiator by total internal reflection. The principal structure of the DIRC in the (x,y,z) coordinate system (bar frame) is illustrated in Fig.7.

Each radiator is a long, thin bar with a rectangular cross section of transverse dimensions (t_x,t_y). When a charged particle passes through the radiator bar, Cherenkov photons are emitted in a conical direction defined by the Cherenkov angle θ_c, where $\cos\theta_c = 1/n\beta$, n is the refractive index. The source length of the emitting region is the particle trajectory length in the radiation material. The angles, positions and momentum of the incident particle are provided by other detectors.

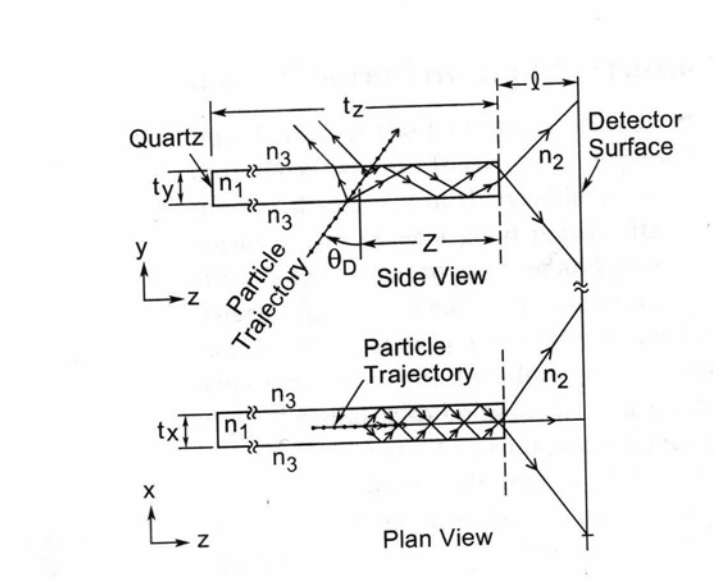

Figure 7: Schematic of a radiator bar of a DIRC counter illustrating the principle of the device. The particle trajectory is shown as a line connected by dots; representative trajectories of Cherenkov photons are shown by lines with arrows.

In the three dimension DIRC concept, the high reflection coefficients inherent in the total internal reflection process and the fact that the magnitudes of angles are conserved during reflection from a flat surface allow the photons of the ring image to be transported to a detector outside the path of the radiating particle, where they may be imaged. Denoting the polar and azimuthal angles of incident charged particles as θ_p and ϕ_p, respectively, the directional cosines of the photon emission in the bar frame can be written as:

$$q_x = -q_{x'}\cos\theta_p\cos\phi_p + q_{y'}\sin\phi_p + q_{z'}\sin\theta_p\cos\phi_p,$$
$$q_y = -q_{x'}\cos\theta_p\cos\phi_p - q_{y'}\cos\phi_p + q_{z'}\sin\theta_p\sin\phi_p,$$
$$q_z = q_{x'}\sin\theta_p + q_{z'}\cos\theta_p,$$

where q_i's(i = x',y',z') are the directional components of the photon emission in the frame where the particle moves along the z'-axis:

$$q_{x'} = \sin\theta_c\cos\phi_c,$$
$$q_{y'} = \sin\theta_c\sin\phi_c,$$
$$q_{z'} = \cos\theta_c.$$

The horizontal and vertical photon angles at the bar end are then given as

$$\Phi = \arctan(q_x/q_z),$$
$$\Theta = \arctan(q_y/q_z).$$

The photon propagates a length (L_p) in a Time-Of-Propagation -TOP (t_p), down a bar length of (L) as is given by $t_p = \frac{L_p n(\lambda)}{c} = \frac{Ln(\lambda)}{cq_z}$,

where $n(\lambda)$ is the refractive index of the radiator at wavelength λ, c is the light velocity in the vacuum, and q_z is the directional z-component of the photon emission.

The azimuthal angle ϕ_c of Cherenkov photons is distributed uniformly over 2π. When one fixes ϕ_c, the individual three-directional components $-q_i$ are uniquely related to θ_c. Therefore, a measurement of any two directional components or any two combinations of them provides information about θ_c. In a DIRC concept the two parameters (Θ,Φ) and time measurement for extracting θ_c are used.

The DIRC prototypes have been constructed and tested over the past. The first large-scale DIRC detector designed for physics is now running in the BABAR detector at PEP-II [15].

A number of DIRC devices have been proposed that use less than three dimensions. For example, a 1-D device called the Cherenkov correlated timing technique - CCT that couples DIRC bars with a non-imaging detection system that times the first photoelectron(s) seen at the bar end was proposed by Aronstain [16]. A prototype has been constructed and tested by Kichimi [17]. The technique uses the correlation between photon path-length and Cherenkov production angle to infer this angle by measuring the time taken for the totally reflected Cherenkov photons to "bounce" to the end of the radiator. This simple principle can be illustrated by the 2-dimensional example shown in Fig. 8. Fig. 8 also demonstrates the difference in flight path for light emitted by π's (thick line) and K's (thin line). Due to this difference the TOP is inversely proportional to z (quartz-axis direction)-component of the light-velocity, which produces TOP differences of, for instance, about 100 ps or more for normal incident 4 GeV/c π and K at 2 m long propagation.

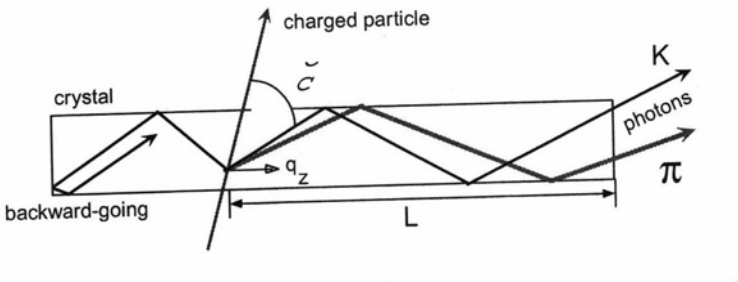

Figure 8**:** Schematic of the Cherenkov correlated timing technique.

Akatsu et al. have proposed and tested [18] a 2-D readout DIRC, one timing dimension - t_p and one space dimension -Φ, called them the time of propagation -TOP counter.

The DIRC counters have confirmed that the Cherenkov radiation images are well transported by internal total reflection, and the CCT counter exhibited that a time measurement of such photons is feasible, while the TOP detector are based on the concept of a 2-D readout DIRC, one timing dimension and one space.

We will consider TOF technique based on the measurement of the time of propagation of Cherenkov photons, similar to the one dimension DIRC- CCT counters, but detection of Cherenkov photons will be carried out by means of RFPP.

3.1 Cherenkov TOP detector: simulation study

Based on the basic concepts considered in the preceding section, we have carried out a simulation study of the proposed technique. In the modeling of the detector the parameters of the radiator are assumed as described in [16, 17]. There are several dominant contributions to the spread of the TOP of the Cherenkov photons in the radiator in addition to the time spread of photon detector:

1) The time spread of Cherenkov radiation along the particle trajectory over the thickness of quartz bar: Cherenkov photons are emitted uniformly along the path of particle passage through the radiator.
2) The transit time spread of Cherenkov photons due to different trajectories: trajectories of the individual photons determined according to θ_c and Φ_c of individual Cherenkov photons.
3) The chromatic effect of Cherenkov light: for the numerical calculations we take $n = 1.47 \pm 0.008$. The Gaussian distribution for n has been used.
4) The timing accuracy of the Photon detector: for the timing accuracy of the Photon detector we take $\sigma = 10$ ps.

The expected total number of photoelectrons- $N_{p.e.}$ detected in the device is: $N_{p.e.} = N_0 \times \Delta l \times (\Delta\Phi_c / 360)$, where $N_0 = 155$ photoelectrons/cm [17] is the Cherenkov quality factor, Δl is the thickness of the radiator, $\Delta\Phi_c$ is the azimuthal angular interval of the detected Cherenkov photons. The size of the radiator bar is 20 mm-thick (in y), 20 mm-wide (in x), and length is in the range 10-200 cm (in z). One end of the Cherenkov radiator is connected to the photon detector, and the opposite end assumed blackened to avoid reflection. So we are considering only forward - FW going photons.

In order to understand the TOP behavior and to evaluate the size of the above effects to TOP and the PID power, a detail calculation has been performed. It has been demonstrated that the results of previous DIRC simulations [18] as well as of the experimental studies [17] are reproduced by our approach with precision better than 20%. Some results are displayed in the Fig.9-Fig.11 and tabulated in Table 1.

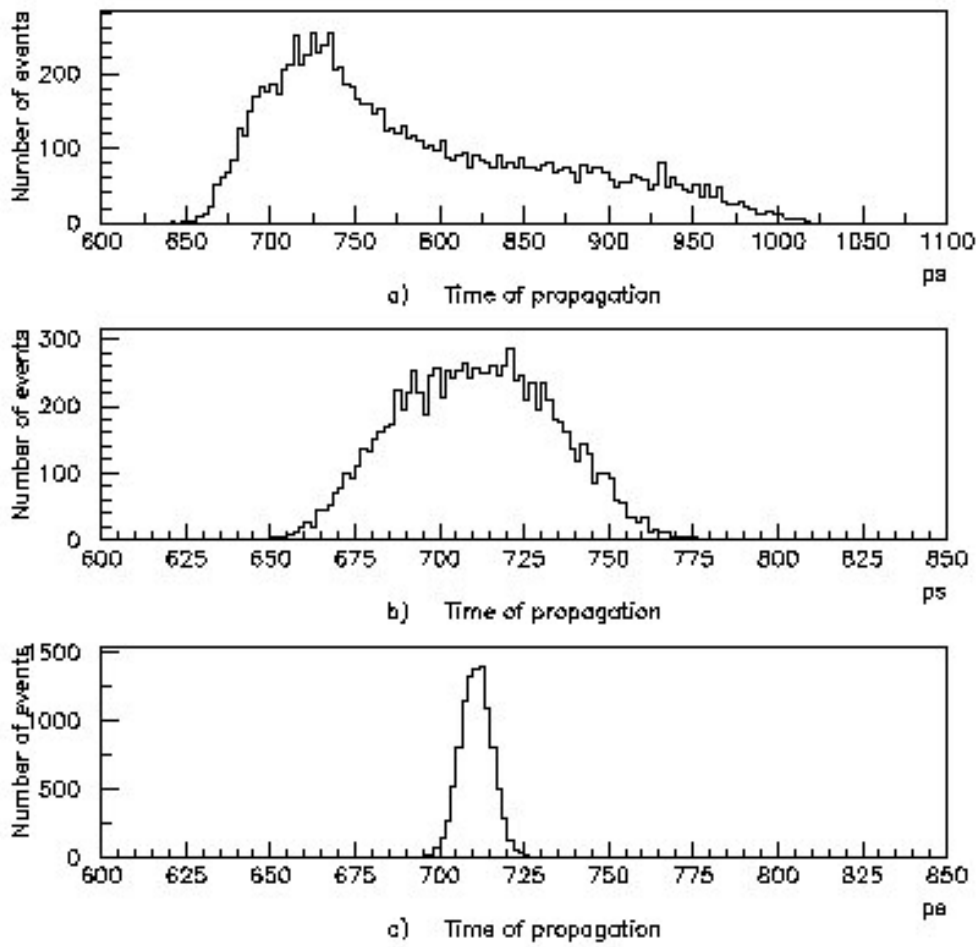

Figure 9: Time of propagation distribution of single and FW going photons for tracks of p = 2 GeV/c pions, $\theta_{inc} = 90^{\circ}$, with $|\Phi_c| \leq 45^{\circ}$ (a), $|\Phi_c| \leq 15^{\circ}$ (b), and mean time distribution of all detected photons (~25) for the case with $|\Phi_c| \leq 15$ (c). The radiator length is L = 10 cm and thickness $\Delta l = 2.0$ cm. For the Cherenkov quality factor we use $N_0 = 155$ p.e./cm [17]. Number of events for each case is equal 10000.

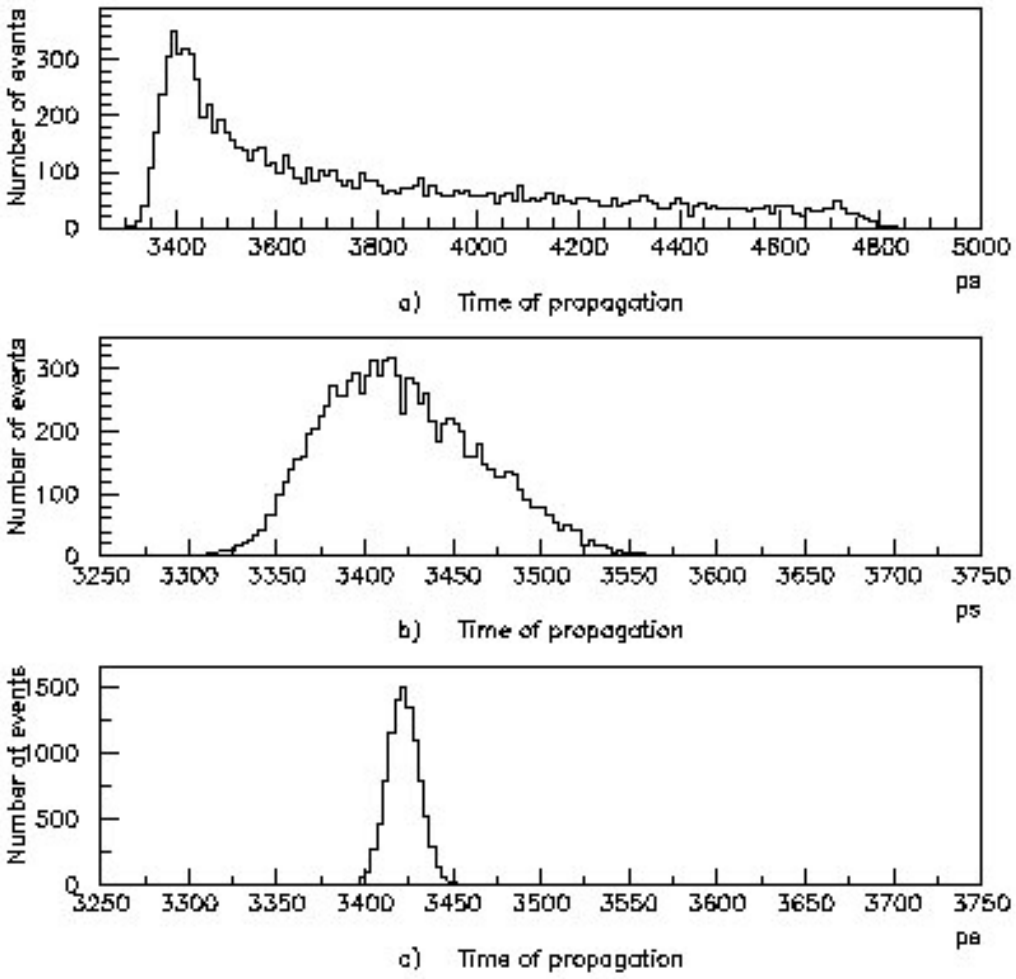

Figure 10: The same as in Fig. 5 but with radiator length L = 50 cm.

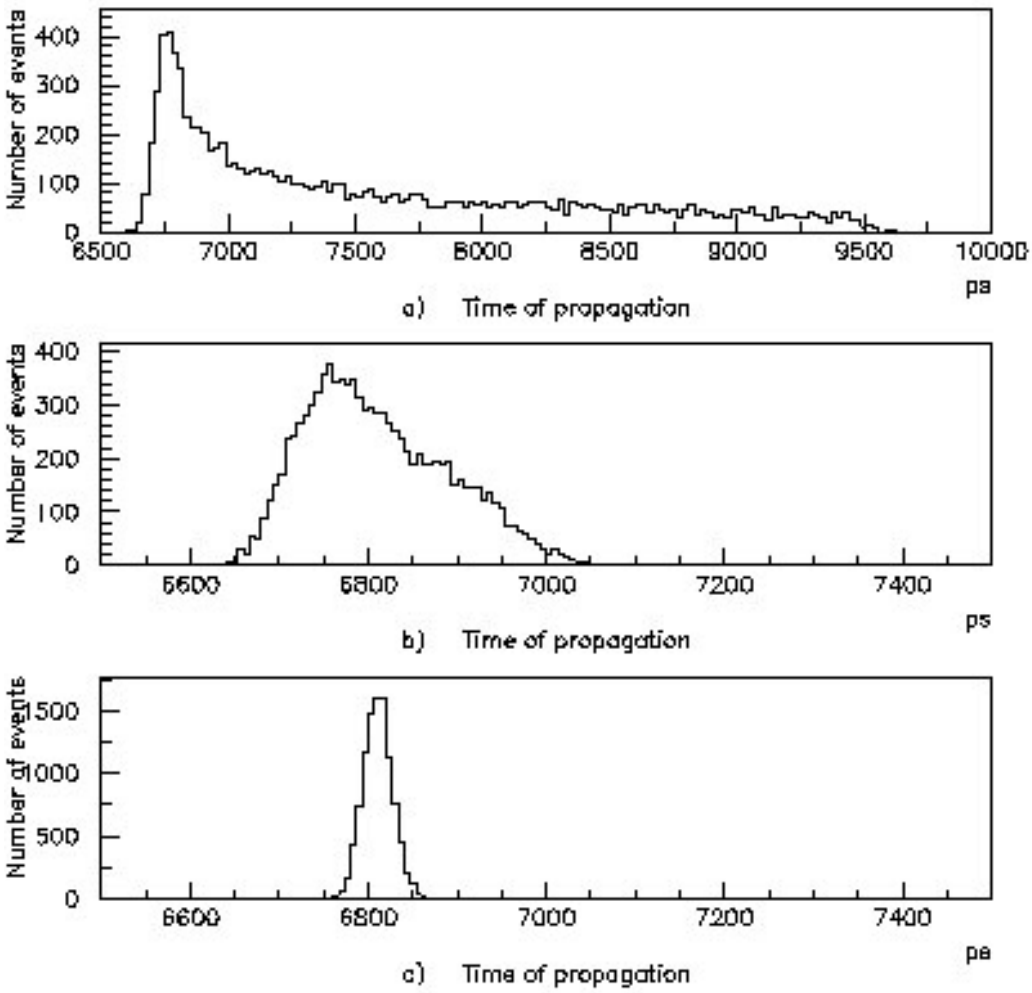

Figure 11: The same as in Fig. 5 but with radiator length L = 100 cm.

Table 1. Average time of propagation and its spread of forward going photons for tracks of p = 2000 MeV/c π and K with $\theta_{inc}=90^{\circ}$, $|\Phi_c| \leq 15^{\circ}$ and for different length L.

L (cm)	20		40		100		200	
Particle	π	K	π	K	π	K	π	K
TOP (ps)	1388	1423	2744	2812	6811	6982	13589	13930
Δ(TOP) (ps)	5.8	6.0	9.0	9.3	20.1	21	40	42
TOP(K) - TOP(π) (ps)	35		68		171		341	

The TOP distributions of 10000 events with 50% π and 50% K tracks of $\theta_{inc}=90^{\circ}$, $|\Phi_c| \leq 15^{\circ}$, L = 100cm and for p = 1.5, 2.0 and 3.0 GeV/c momentum are displayed in Fig.8. The number of σ separation N_σ between π/K of p = 2 GeV/c momentum and with

L = 100 cm is about 8.5. It is interesting to compare with results of the 3D DIRC. For a particle of momentum p well above threshold entering a radiator with index of refraction n, the number of σ separation N_σ between particles of mass m_1 and m_2 in the 3D DIRC is approximately [26]:

$$N_\sigma \approx \frac{\left|m^2{}_1 - m^2{}_2\right|}{2p^2\sigma[\theta_c(tot)]\sqrt{n^2-1}}.$$

For the N_σ = 8.5 separation, the $\sigma[\theta_c(tot)]$ must be about 3 mrad, for n = 1.47 radiator. In the practical 3D DIRC counters, the attainable angular resolution $\sigma[\theta_c(tot)]$ varies between 0.5 and 5 mrad [26].

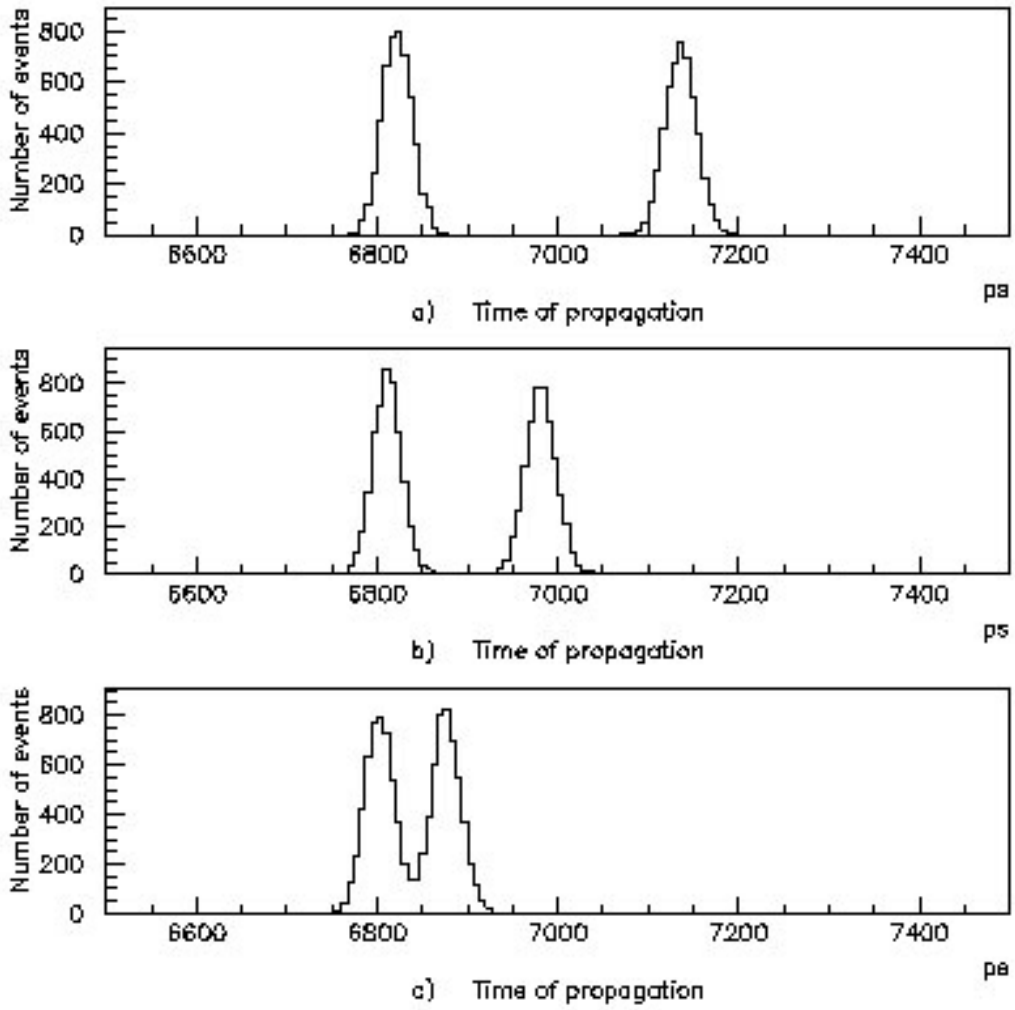

Figure 12**:** Average time of propagation distributions for forward going photons with $|\Phi_c| \le 15^\circ$ and L = 100 cm, for π (left histograms) and K (right histograms), $\theta_{inc}=90^\circ$ and p =1.5 (a), 2.0 (b), 3.0 (c) GeV/c momentum. Total number of events is 10000 with 50% π and 50% K tracks.

These simulations have demonstrated that such a simple and compact TOP Cherenkov counter can be used for π and K separation in the 1-3 GeV/c momentum range. The differences of TOF between π and K are 231 and 37 ps at 10 m time-of-flight

distance and for p = 4 and 10 GeV/c, respectively, and by using 40 cm length Cherenkov detector based on the picosecond photon detector, about 25σ and 4σ π/K separation can be reached for p = 4 and 10 GeV/c, respectively.

3.2 Cherenkov TOP (CCT) detector: practical issues

Practical realization of the Cherenkov TOP detector is possible by using the RF phototube with direct readout scheme. By using direct readout scheme such as an array of small ($\sim 1mm^2$) pixels with one readout channel per pixel, the RFPP can be used to digitize the Cherenkov photon pulse, i.e. to detect each Cherenkov photon and measure its arrival time.

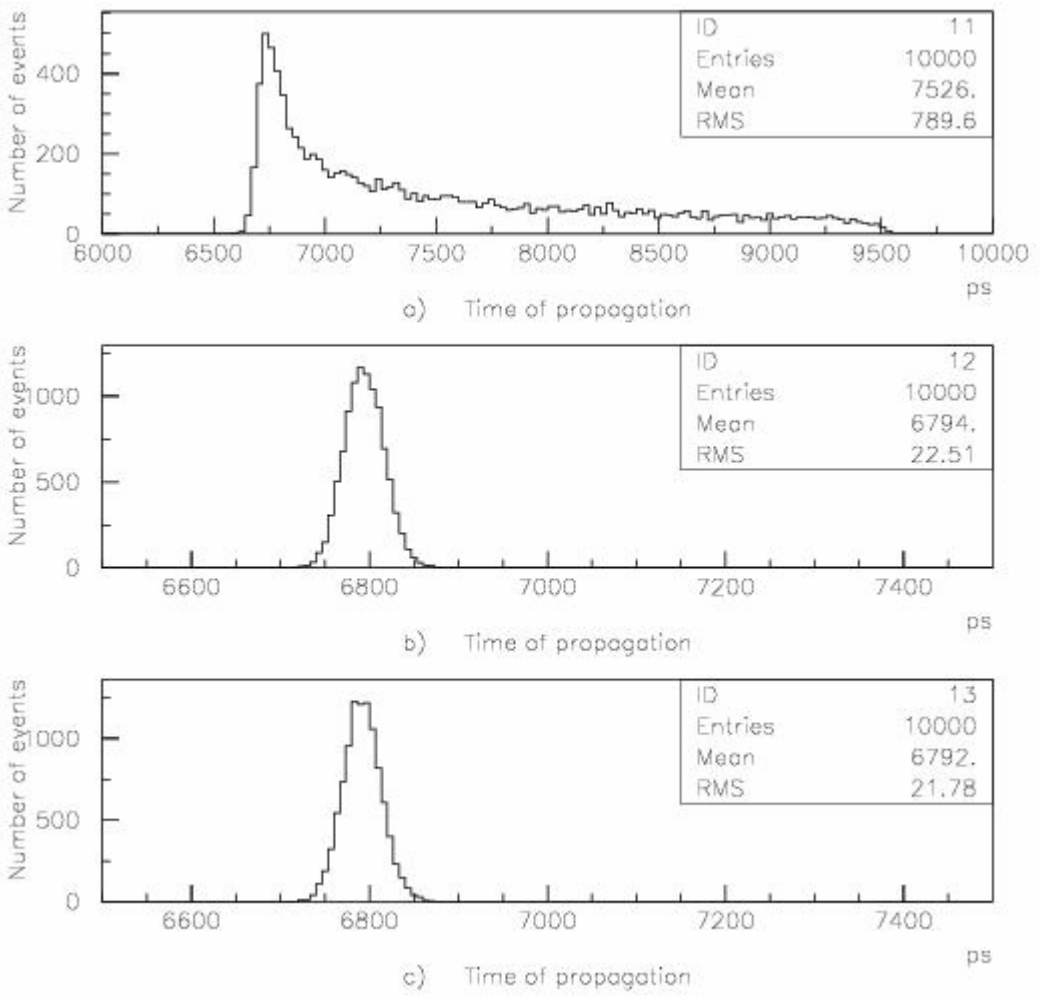

Figure 13: Time of propagation distribution of single and FW going photons for tracks of p = 2 GeV/c pions, $\theta_{inc} = 90^\circ$, with $|\Phi_c| \le 45^\circ$ (a), and mean time distribution of all detected photons for the cases with $|\Phi_c| \le 15^\circ$ (b) and $t \le 6950$ ps (c). The radiator length is L = 100 cm and thickness Δl = 1.0 cm. For the Cherenkov quality factor we use $N_0 = 155$ p.e./cm [17]. Number of events for each case is equal 10000.

Due to strong correlation between arrival times of Cherenkov photons and azimuthal angles- Φ_c (see Fig.9[a,b], Fig.10[a,b], Fig.11[a,b]), instead of restricted Φ_c intervals we can use restricted time intervals. The time of propagation distribution of single and FW going photons for tracks of p = 2 GeV/c pions, $\theta_{inc} = 90^\circ$, with $|\Phi_c| \le 45^\circ$ (a), and the average time distribution of detected photons with $|\Phi_c| \le 15$ (b) or with arrival times less than $t \le 6950$ ps, obtained as a result of Monte Carlo simulation, is shown in Fig. 13[a,b,c]. The radiator length is L = 100 cm and thickness $\Delta l = 1.0$ cm. As follows from Fig.13[b] and Fig.13[c], restriction of azimuthal angles - Φ_c or arrival times of Cherenkov photons are equivalent and result the same average time distribution. Therefore by using RFPP with direct readout scheme, the time information for each detected event can be reconstructed by means of software analysis. Such a CCT (TOP) Cherenkov detector can be used at JLab in all three Halls especially in the future 12 GeV program to identify particle types.

3.3 Cherenkov TOF detector in a "head-on" geometry

Here we will consider Cherenekov detector in "head-on" geometry type, schematically shown in Fig. 14. In such a simple and technically durable design the transit time spread of photons is the same for all Φ_c, at least for the particles incident nearly normal to the radiator. We have carried out a simulation study of timing characteristics of such type of detector by using Monte Carlo code. We take into account the following factors:

1. The time spread of Cherenkov radiation along the particle trajectory over the thickness of quartz radiator: Cherenkov photons are emitted uniformly along the path of particle passage through the radiator.
2. The transit time spread of Cherenkov photons due to different trajectories: trajectories of the individual photons determined according to θ_c and Φ_c of individual Cherenkov photons.
3. The chromatic effect of Cherenkov light: for numerical calculations we take $n = 1.47 \pm 0.008$. A Gaussian distribution for n has been used.
4. The timing accuracy of the photon detector: for the timing accuracy of the photon detector we take $\sigma = 15$ ps and Gaussian distribution has been used.

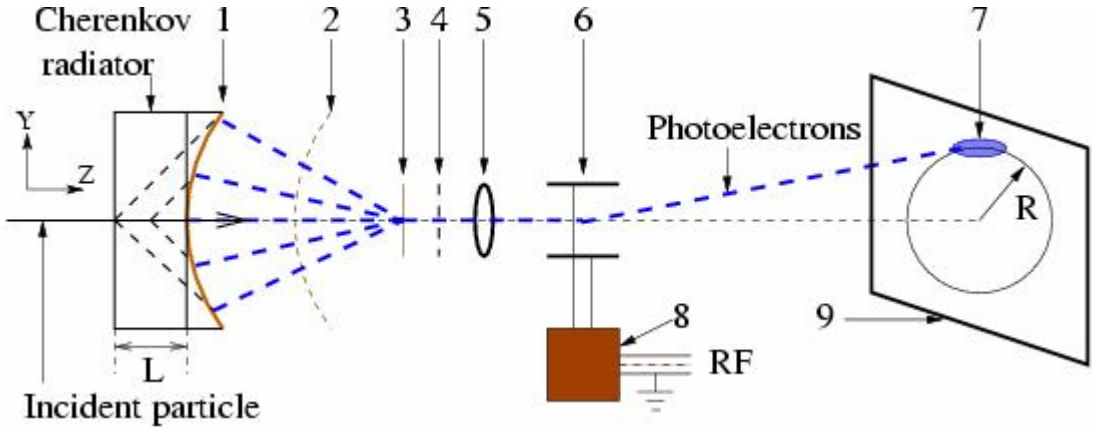

Figure 14: The schematic layout of the Cherenkov TOF detector with RF phototube in a "head-on" geometry (for notations see Fig. 6)

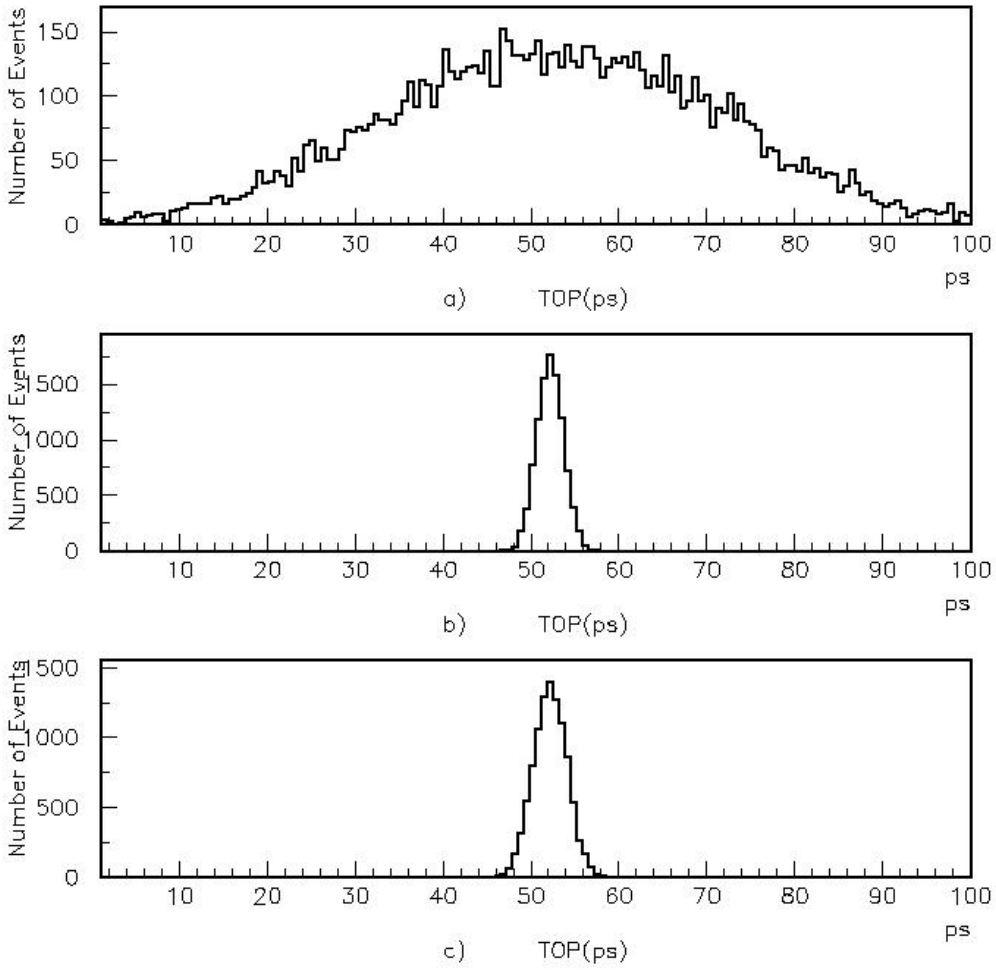

Figure 15: Time of propagation (TOP) distribution of single photoelectrons for tracks of p = 5000 MeV/c pions (a), and mean TOP distribution of all detected photons for $N_0 = 155$ cm^{-1} (b) and $N_0 = 100$ cm^{-1} (c) cases. Number of events for each case is equal 10000.

The expected total number of photoelectrons $N_{p.e.}$ detected in the device is: $N_{pe} = N_0 \times \Delta l$, where $N_0 = 155\,\text{cm}^{-1}$ [16] is the Cherenkov quality factor, Δl is the thickness of the radiator. Results for the normally incident 5000 MeV/c pions and for quartz radiator, $n = 1.47$ and $\Delta l = 1.0$ cm are displayed in the Fig. 15. These simulations have demonstrated that such a Cherenkov detector can provide time resolution better than 5 ps FWHM. An array of such detectors, Cherenkov TOF wall, schematically displayed in the Fig. 16 can be used as a particle identification device for JLab's 12 GeV program.

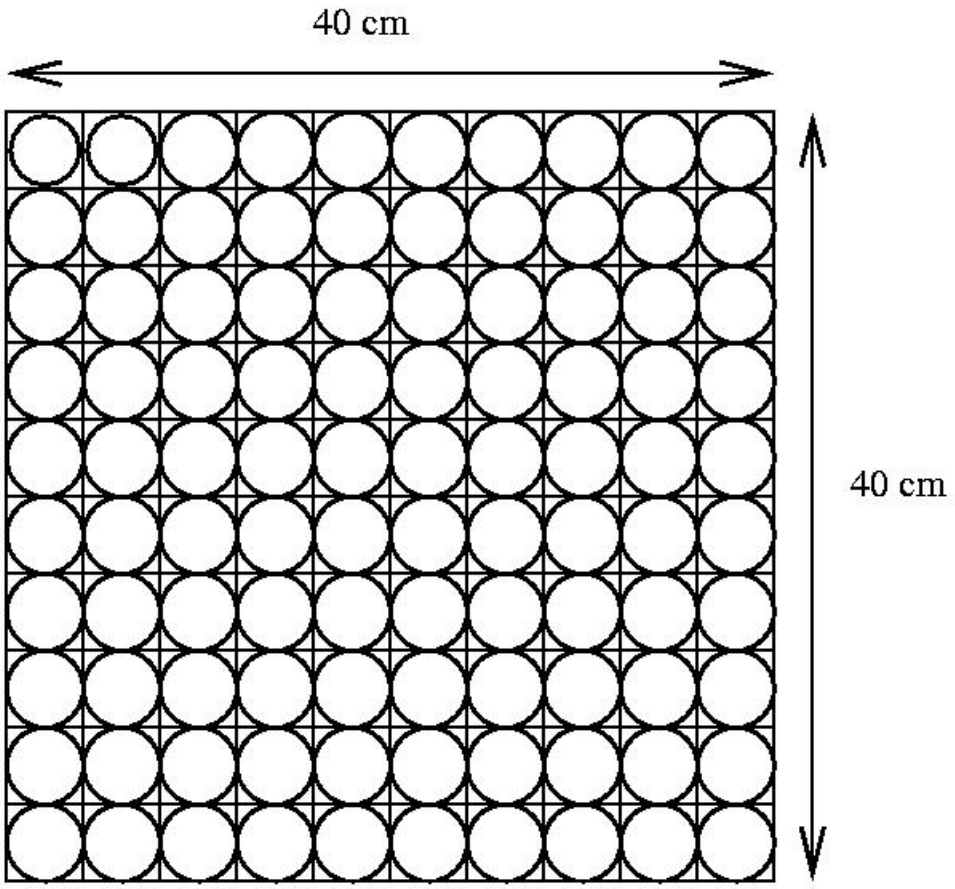

Figure 16: The schematic layout of the Cherenkov TOF wall.

4. An overview of the RF Cherenkov picosecond TOF program

We define the project with three following phases:

1. Phase 1: R&D for optimization of the parameters of 500 MHz RFPP, construction of real prototype of the RFPP and technology development for manufacturing of the RFPP. These investigations are planned to carry out at the Yerevan, Tohuku University and JLab in close collaboration with US manufacturing company.
2. Phase 2: Development and construction of the Cherenkov TOF detectors based on the RFPP. The prototypes of the Cherenkov TOF detectors will be constructed and tested at Yerevan by using pulsed light sources and cosmic rays, at Tohoku University electron stretcher booster, and latter at JLab. The time structure of the Tohoku University electron stretcher booster is same (500 MHz) as the time structure of electron beams in the JLab experimental Halls.
3. Phase 3: Construction and test of the RF Cherenkov picosecond TOF detectors. We are planning to develop and construct RF Cherenkov TOF technique for hypernuclear studies at JLab.

5. Conclusions

The approval of this Project will be used to continue R&D for optimization and manufacturing of the RFPP and for development of the Cherenkov picosecond detectors based on the RFPP for JLab 12 GeV physics program.

We propose two type of Cherenkov time of flight technique based on the RFPP:

a) Cherenkov correlated timing detector or time of propagation detector;
b) Cherenkov TOF detector in a “head-on” geometry.

The final goal of this Project is a construction of the RF Cherenkov detectors for hypernuclear studies at JLab.

The developed RFPP can find applications in other fields, e.g. in medical imaging such as time resolved diffuse optic tomography, fast fluorescence spectroscopy, laser ranging, etc.

References

[1] M. Akatsu et al., MCP-PMT timing property for single photons, Nucl. Instr. And Meth. A528 (2004)763

[2] E. K. Zavoisky and S. D. Fanchenko, Physical principles of electron-optical chronography, Sov. Phys. Doklady 1 (1956) 285.

[3] D. J. Bradly, Ultrashort Light Pulses, Picosecond Techniques and Applications, in Topics in Applied Physics, 18 (1977) 17.

[4] A. M. Prokhorov and M. Ya. Schelev, Recent research and development in electron image tubes/cameras/systems, International Congress on High-Speed Photography and Photonics, Proc. SPIE 1358 (1990) 280.

[5] K. Scheidt, Review of Streak Cameras for Accelerators: Features, Applications and Results, Proceedings of EPAC 2000, Vienna (2000) 182.

[6] Wilfried Uhring et al., Very high long-term stability synchroscan streak camera, Rev. Sci. Instrum. 74 (2003) 2646.

[7] R. Carlini, N. Grigoryan, O. Hashimoto et al., Proposal for Photon Detector with Picosecond Resolution, H. Wiedemann (ed), Advanced Radiation Sources and Applications, NATO Science Series, 199, Springer, 2006, 305.

[8] A. Margaryan, R. Carlini, R. Ent et al., Radio frequency picosecond phototube, Nucl. Instrum. and Meth. A566 (2006) 321.

[9] G. I. Bryukhnevitch, S. A. Kaidalov, V. V. Orlov, A. M. Prokhorov et all., PV006S Streak Tube For 500 MHz Circular-Scan Operation, Electron Tubes and Image Intensifiers, Proc. SPIE 1655 (1992) 143.

[10] Boris. E. Dashevsky, New electron optic for high-speed single-frame and streak image intensifier tubes, Proc. SPIE 1358 (1990) 561.

[11] E. W. Ernst and H. VonFoerster, Time Dispersion of Secondary Electron Emission, Appl. Phys. 26 (1955) 781.

[12] I. M. Frank, Vavilov-Cherenkov Radiation. Theoretical Aspects. In Russian. "Nauka" Moscow, 1988, pp. 204-247.

[13] S. Majewski, A. Margaryan, L. Tang, Proposal for Cherenkov time of flight technique with picosecond resolution, 2005, e-Print Archive: physics/0508040.

[14] Blair N. Ratcliff, "Imaging rings in Ring Imaging Cherenkov counters", Nucl. Instrum. and Methods A 502, (2003) 211.

[15] David W.G.S. Leith, DIRC-the identification system for BaBar, Nucl. Instrum. and Methods A 494, (2002) 389.

[16] D. Aronstein et al., The Cherenkov correlated timing detector: materials, geometry and timing constraints, Nucl. Instrum. and Meth. A 371 (1996) 87.

[17] H. Kichimi et al., The Cherenkov correlated timing detector: beam test results from quartz and acrylic bars, Nucl. Instrum. and Meth. A 371 (1996) 91.

[18] H. M. Akatsu et al., Time-of-propagation Cherenkov counter for particle identification, Nucl. Instrum. and Methods A 440, (2000) 124.